studies are needed to examine changes in PCL laxity due to degeneration or attenuation with time. Flexion instability due to late PCL insufficiency could be a cause of persistent pain and functional impairment after CR TKA leading to revision arthroplasty.[35–37] Frequent kneeling may cause a dysfunction of the retained PCL after CR TKA and the post-cam mechanism after PS TKA over time because the retained PCL and the post-cam mechanism receive significant load.

Our study has limitations. Kinematic information concerning deep knee flexion could not be included in the analysis because most of the subjects could not kneel beyond 130°. Both CR and PS designs used in this study are not intended to flex beyond 130°. More research is needed to assess the dynamic in vivo function of the PCL and the post-cam mechanism in deep flexion.

In conclusion, our results suggest that the PCL after CR TKA and the post-cam mechanism after PS TKA function during kneeling from 90 to 120° of knee flexion. Based on our results, PS TKA may be preferable to CR TKA to reduce forces across the patellofemoral articulation. The PS design has contact regions located far posterior on the tibial insert in comparison to the CR TKA. Specifically, the lateral femoral condyle in PS TKA translated to the posterior edge of the tibial surface. Furthermore, this study suggests the hypothesis that increased edge loading may be associated with an abnormally high degree of stress in the polyethylene, and that this may be associated with an increased risk of failure. Only a clinical study with long term follow-up can determine if this relationship exists, but further attention must be given to the configuration of the post-cam when designing posterior-stabilized total knee prostheses.

ACKNOWLEDGMENTS

No benefits in any form were received from a commercial party related directly or indirectly to the subject of this article.

REFERENCES

1. Weiss JM, Noble PC, Conditt MA, et al. 2002. What functional activities are important to patients with knee replacements? Clin Orthop 404:172–188.
2. Palmer SH, Servant CT, Maguire J, et al. 2002. Ability to kneel after total knee replacement. J Bone Joint Surg Br 84:220–222.
3. Hassaballa M, Vale T, Weeg N, et al. 2002. Kneeling requirements and arthroplasty surgery. Knee 9:317–319.
4. Berg P, Mjoberg B. 1991. A lateral skin incision reduces peripatellar dysaesthesia after knee surgery. J Bone Joint Surg Br 73:374–376.
5. Schai PA, Gibbon AJ, Scott RD. 1999. Kneeling ability after total knee arthroplasty. Perception and reality. Clin Orthop 367:195–200.
6. Dahlkvist NJ, Mayo P, Seedhom BB. 1982. Forces during squatting and rising from a deep squat. Eng Med 11:69–76.
7. Toutoungi DE, Lu TW, Leardini A, et al. 2000. Cruciate ligament forces in the human knee during rehabilitation exercises. Clin Biomech 15:176–177.
8. Nagura T, Dyrby CO, Alexander EJ, et al. 2002. Mechanical loads at the knee joint during deep flexion. J Orthop Res 20:881–886.
9. Komistek RD, Scott RD, Dennis DA, et al. 2002. In vivo comparison of femorotibial contact positions for press-fit posterior stabilized and posterior cruciate-retaining total knee arthroplasties. J Arthroplasty 17:209–216.
10. Incavo SJ, Mullins ER, Coughlin KM, et al. 2004. Tibiofemoral kinematic analysis of kneeling after total knee arthroplasty. J Arthroplasty 19:906–910.
11. Nakayama K, Matsuda S, Miura H, et al. 2005. Contact stress at the post-cam mechanism in posterior-stabilized total knee arthroplasty. J Bone Joint Surg Br 87:483–488.
12. Garling EH, Kaptein BL, Geleijns K, et al. 2005. Marker configuration model-based roentgen fluoroscopic analysis. J Biomech 38:893–901.
13. Fukuoka Y, Hoshino A, Ishida A. 1999. A simple radiographic measurement method for polyethylene wear in total knee arthroplasty. IEEE Trans Rehabil Eng 7:228–233.
14. Banks SA, Hodge WA. 1996. Accurate measurement of three-dimensional knee replacement kinematics using single-plane fluoroscopy. IEEE Trans Biomed Eng 43:638–649.
15. Higaki H, Shimoto T, Miura H, et al. 2002. Application of pattern matching method in motion analysis for TKA. Trans Jpn Soc Mech Eng 68:3061–3068.
16. Shimoto T, Higaki H, Hukunaga T, et al. 2003. Study of the motion analysis for total knee arthroplasty using flat panel detector. Proceedings of the IASTED International Conference on Biomechanics. Calgary, Canada: ACTA Press; p 28–33.
17. Hazaki S, Yokoyama Y, Inoue H. 2001. A radiographic analysis of anterior–posterior translation in total knee arthroplasty. J Orthop Sci 6:390–396.
18. Bertin KC, Komistek RD, Dennis DA, et al. 2002. In vivo determination of posterior femoral rollback for subjects having a NexGen posterior cruciate-retaining total knee arthroplasty. J Arthroplasty 17:1040–1048.
19. Nozaki H, Banks SA, Suguro T, et al. 2002. Observations of femoral rollback in cruciate-retaining knee arthroplasty. Clin Orthop 404:308–314.
20. Most E, Zayontz S, Li G, et al. 2003. Femoral rollback after cruciate-retaining and stabilizing total knee arthroplasty. Clin Orthop 410:101–113.
21. Churchill DL, Incavo SJ, Johnson CC, et al. 2001. The influence of femoral rollback on patellofemoral contact loads in total knee arthroplasty. J Arthroplasty 16:909–918.
22. Browne C, Hermida JC, Bergula A, et al. 2005. Patellofemoral forces after total knee arthroplasty: effect of extensor moment arm. Knee 12:81–88.
23. Wasielewski RC, Galante JO, Leighty RM, et al. 1994. Wear patterns on retrieved polyethylene tibial inserts and

their relationship to technical considerations during total knee arthroplasty. Clin Orthop 299:31–43.
24. Harman MK, Banks SA, Hodge WA. 2001. Polyethylene damage and knee kinematics after total knee arthroplasty. Clin Orthop 392:383–393.
25. Gidwani S, Langkamer VG. 2001. Recurrent dislocation of a posterior-stabilized prosthesis: a series of three cases. Knee 8:317–320.
26. Ochsner JL Jr, Kostman WC, Dodson M. 1996. Posterior dislocation of a posterior-stabilized total knee arthroplasty. A report of two cases. Am J Orthop 25:310–312.
27. Petrie RS, Trousdale RT, Cabanela ME. 2000. Total knee arthroplasty for chronic posterior knee dislocation: report of 2 cases with technical considerations. J Arthroplasty 15:380–386.
28. Su YP, Chiu FY, Chen TH. 2003. Posterior dislocation after posterior stabilization TKA. J Chin Med Assoc 66:120–122.
29. Clarke HD, Math KR, Scuderi GR. 2004. Polyethylene post failure in posterior stabilized total knee arthroplasty. J Arthroplasty 19:652–657.
30. Hendel D, Garti A, Weisbort M. 2003. Fracture of the central polyethylene tibial spine in posterior stabilized total knee arthroplasty. J Arthroplasty 18:672–674.
31. Mestha P, Shenava Y, D'Arcy JC. 2000. Fracture of the polyethylene tibial post in posterior stabilized (Insall Burstein II) total knee arthroplasty. J Arthroplasty 15:814–815.
32. Ng TP, Chiu KY. 2003. Recurrent dislocation of total knee arthroplasty: an unusual cause. J Arthroplasty 18:1067–1070.
33. Puloski SK, McCalden RW, MacDonald SJ, et al. 2001. Tibial post wear in posterior stabilized total knee arthroplasty. An unrecognized source of polyethylene debris. J Bone Joint Surg Am 83:390–397.
34. Andriacchi TP, Galante JO. 1988. Retention of the posterior cruciate in total knee arthroplasty. J Arthroplasty 3 (Suppl):S13–S19.
35. Montgomery RL, Goodman SB, Csongradi J. 1993. Late rupture of the posterior cruciate ligament after total knee replacement. Iowa Orthop J 13:167–170.
36. Pagnano MW, Hanssen AD, Lewallen DG, et al. 1998. Flexion instability after primary posterior cruciate retaining total knee arthroplasty. Clin Orthop 356:39–46.
37. Wang CJ, Wang HE. 1997. Dislocation of total knee arthroplasty. A report of 6 cases with 2 patterns of instability. Acta Orthop Scand 68:282–285.

Three-Dimensional Knee Joint Kinematics during Golf Swing and Stationary Cycling after Total Knee Arthroplasty

Satoshi Hamai,[1] Hiromasa Miura,[1] Hidehiko Higaki,[2] Takeshi Shimoto,[2] Shuichi Matsuda,[1] Ken Okazaki,[1] Yukihide Iwamoto[1]

[1]Department of Orthopaedic Surgery, Graduate School of Medical Sciences, Kyushu University, 3-1-1 Maidashi, Higashi-ku, Fukuoka 812-8582, Japan, [2]Department of Mechanical Engineering, Faculty of Engineering, Kyushu Sangyo University, 2-3-1 Matsugadai, Higashi-ku, Fukuoka 813-8583, Japan

Received 4 October 2007; accepted 25 February 2008
Published online 3 June 2008 in Wiley InterScience (www.interscience.wiley.com). DOI 10.1002/jor.20671

ABSTRACT: The expectation of returning to sports activities after total knee arthroplasty (TKA) has become more important to patients than ever. To our knowledge, no studies have been published evaluating the three-dimensional knee joint kinematics during sports activity after TKA. Continuous X-ray images of the golf swing and stationary cycling were taken using a large flat panel detector for four and eight post-arthroplasty knees, respectively. The implant flexion and axial rotation angles were determined using a radiographic-based, image-matching technique. Both the golf swing from the set-up position to the top of the backswing, and the stationary cycling from the top position of the crank to the bottom position of the crank, produced progressive axial rotational motions ($p = 0.73$). However, the golf swing from the top of the backswing to the end of the follow-through produced significantly larger magnitudes of rotational motions in comparison to stationary cycling ($p < 0.01$). Excessive internal–external rotations generated from the top of the backswing to the end of the follow-through could contribute to accelerated polyethylene wear. However, gradual rotational movements were consistently demonstrated during the stationary cycling. Therefore, stationary cycling is recommended rather than playing golf for patients following a TKA who wish to remain physically active. © 2008 Orthopaedic Research Society. Published by Wiley Periodicals, Inc. J Orthop Res 26:1556–1561, 2008

Keywords: golf swing; stationary cycling; total knee arthroplasty; image-matching technique

Total knee arthroplasty (TKA) provides excellent pain relief, correction of deformity, and improved function.[1–3] The improvement in pain and function allows some patients to participate in sports activities. The goals and expectations of patients undergoing TKA tend to vary greatly, depending on lifestyle. However, the expectations of returning to sports have become more important to patients than ever before.[4,5] In addition, physical fitness and exercise are associated with improved muscle strength and coordination,[6,7] increased flexibility,[6,8] weight reduction,[9,10] lowering of systemic blood pressure, and prevention of cardiac problems.[10,11] Furthermore, regular exercise has positive effects on total joint arthroplasty, such as an improved bone quality and implant fixation.[12–14] However, orthopedic surgeons have concerns about the risk for aseptic loosening due to polyethylene wear and debris.[15,16] Thus, most studies recommend participation in low-impact sports such as swimming, regular walking, cycling, bowling, sailing, scuba diving, and golf.[4,14,17,18] High-impact sports, such as running, football, baseball, basketball, hockey, handball, karate, soccer, and racquetball, are not recommended after total joint arthroplasty. The risks of prosthetic wear, dislocation, and periprosthetic fracture may increase with high-impact sports. However, the recommendations in the literature are mainly based upon the subjective opinions of surgeons. Little scientific evidence exists supporting such recommendations.

Golf is a popular recreational sport played more frequently among seniors in whom TKAs are usually performed.[4] A previous study reported that 39% of patients undergoing TKA considered golf important and 18% played golf.[5] Patients have considerable interest, but also have concerns about the risks and benefits of playing golf after joint replacement. Members of the Knee Society usually do not discourage their TKA patients from playing golf.[19] However, significant rotational torque around the knee occurs at very high speeds during the golf swing.[20] Despite the fact that golf is considered a low-impact sport, concerns exist about whether a golf swing can be performed in a safe manner after TKA. Stationary cycling is another low-impact sport. The knee moment induced during cycling is small compared to that induced during other exercises, or normal activities such as walking and stair climbing.[21] Therefore, the stationary bike has been widely used in rehabilitation after knee joint surgery and in various dysfunctions of the lower limb.[22] A previous study reported that many patients (51% of those studied) regularly participated in stationary cycling.[5] In comparison to activities that placed greater loads on the extremities or demanded increased knee flexion, few patients (15%) reported that their TKA caused moderate to severe difficulty when performing stationary cycling.

Our purpose was to clarify in vivo kinematics during golf swing and stationary cycling after TKA using radiographic-based, image-matching techniques. Previous in vivo fluoroscopic studies focused on kinematic information during daily activities such as normal gait,[23,24] stair climbing,[25] deep knee bend,[23–25] and kneeling.[26] To our knowledge, no study has been published evaluating 3-D knee joint kinematics during sports activity after TKA.

METHODS

The study group consisted of eight patients with 12 primary TKAs with a minimum follow-up of 6 months and no other joint arthroplasties. All subjects provided written consent for this

Correspondence to: Hiromasa Miura (T: +81-92-642-5488; F: +81-92-642-5507; E-mail: miura@ortho.med.kyushu-u.ac.jp)

institutional review board-approved study. The subjects were still playing golf or stationary cycling and were analyzed either during golf swinging or stationary cycling under radiographic surveillance using a flat panel detector (Hitachi, Clavis, Tokyo, Japan: 3 frames per second, image area size 397 (H) × 298 (V) mm, and 0.20 × 0.20 mm/pixel resolution). Two designs were used: a cruciate-retaining TKA (Foundation, Encore Medical, Austin, TX) and a posterior-stabilized TKA (Nexgen LPS Flex, Zimmer, Warsaw, IN). The articulating surface geometry of the polyethylene insert is designed to allow ±9° internal–external rotation in the cruciate-retaining TKA and ±12° in the posterior-stabilized TKA.

During golf swing, four knees in four subjects were analyzed, one woman and three men, averaging 73 ± 8 years (range, 63–81). The preoperative diagnoses were osteoarthritis in all knees. One knee received a cruciate-retaining TKA, the others a posterior-stabilized TKA. The average age at the time of TKA was 71 ± 8 years (range, 61–80), and the average follow-up was 22 ± 3 months (range, 17–25). The postoperative knee extension/flexion angle was 0 ± 0° (range, 0 to 0)/125 ± 27° (range, 115–130). The knee score/function score was 97 ± 5 (range, 90–100)/85 ± 13 (range, 70–100) based on the Knee Society Clinical Rating System. All the subjects were right-handed recreational golfers. Three trail knees (the right knee in the right-handed golfer) and one lead knee (the left knee in the right-handed golfer) were analyzed; the subjects wore soft-spike golf shoes. The subjects stood in their normal golf stance with the arthroplasty knee on a flat panel detector (Fig. 1A). Subjects were allowed to adjust their stance until they felt comfortable and to warm up sufficiently before data collection. Five X-ray images from the set-up position to the end of the follow-through (set-up, early backswing, late backswing, top of the backswing, and end of the follow-through) were analyzed using image-matching techniques.

During stationary cycling, eight knees in six subjects were analyzed. These eight knees included seven women and one man, averaging 68 ± 10 years (range, 56–84). Three knees received a cruciate-retaining TKA, and five knees received a posterior-stabilized TKA. The preoperative diagnoses were osteoarthritis in all knees. The age at TKA was 66 ± 10 years (range, 55–82), and the follow-up after surgery was 20 ± 6 months (range, 10–27). The postoperative knee extension/flexion angle was −6 ± 10° (range, −25 to 0)/121 ± 11° (range, 105–135). The knee score/function score was 92 ± 6 (range, 80–99)/91 ± 10 (range, 70–100) based on the Knee Society Clinical Rating System. The subjects were not cycling experts, only riding occasionally prior to surgery. The subjects pedaled a stationary bike (AF6500, ALINCO Inc, Osaka, Japan) at rates of 20 rpm, a work rate of 35 Watts (Fig. 1B). All subjects were allowed to adjust the saddle height and to warm up before data

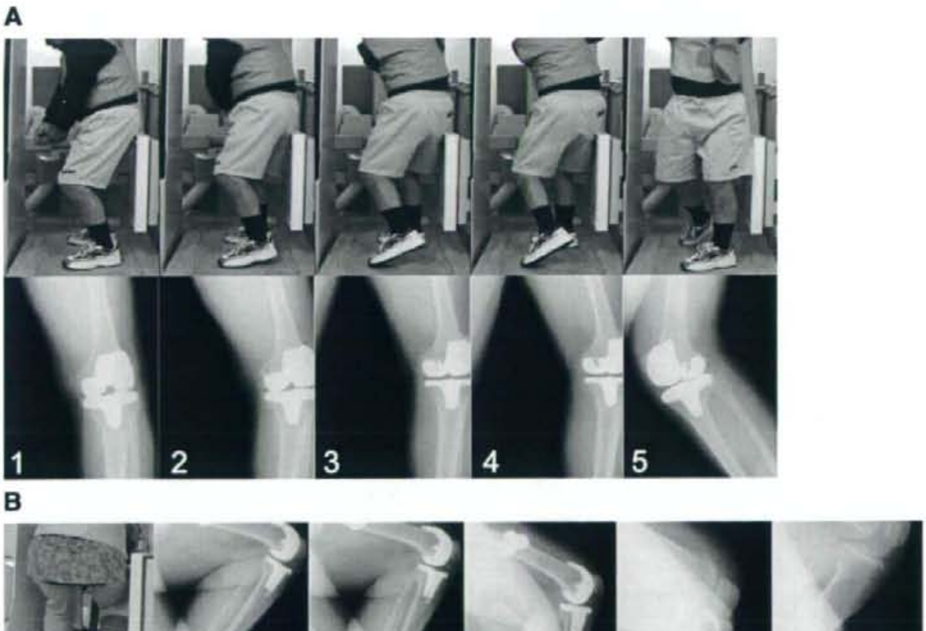

Figure 1. (A) A right-handed subject performed a golf swing (upper stand) while their knee motion was observed using a large flat-panel X-ray image detector. The X-ray images (lower stand) showed the trail (right) knee being studied. Five X-ray images, analyzed using radiographic-based, image-matching techniques were: (1) set-up, (2) early backswing, (3) late backswing, (4) top of the backswing, and (5) end of the follow-through. (B) Each subject performed cycling on a stationary bike at 20 rpm (left) while their knee motion was observed using a large flat-panel X-ray image detector. Continuous X-ray images, taken at 3 frames per second, show the right knee from the top position of the crank to the bottom position being studied: (1) top position, (2) 25% phase, (3) 50% phase, (4) 75% phase, and (5) bottom position.

collection. The subjects maintained the pedaling rate by observing a digital display. The stationary bike was set 10° obliquely to a flat panel detector to prevent obscure images from the contralateral leg. Five X-ray images from the top position of the crank to the bottom position (top position, 25% phase, 50% phase, 75% phase, and bottom position) were analyzed using image-matching techniques.

A model silhouette was matched with the actual object silhouette by translating and rotating the 3-D model to minimize the number of unmatched pixels between both silhouettes. After the 3-D poses of the femoral and tibial components were estimated, the six degrees-of-freedom of the femoral component relative to the tibial component were determined by transforming the coordinate systems into one common system. The root-mean-square errors for this process at the femoral component were 0.29 mm for in-plane translation, 0.37 mm for out-of-plane translation, and 0.27° for rotation; at the tibial component, they were 0.23 mm for in-plane translation, 0.30 mm for out-of-plane translation, and 0.25° for rotation.[26] The implant flexion and axial rotation angles were determined during both golf swing and stationary cycling. The positive or negative value of implant flexion was defined as flexion or extension of the femoral component relative to the tibial component. The positive or negative value of implant rotation was defined as the internal or external rotation of the femoral component relative to the tibial component.

Values were expressed as the mean ± standard deviation. Mann–Whitney's U test was used to analyze the absolute value of the rotational motion in comparing the golf swing (from the set-up position to the top of the backswing and from the top of the backswing to the end of the follow-through) with stationary cycling. Probability values <0.05 were considered significant.

RESULTS

Golf Swing

The subject undergoing TKA in the lead knee had the following implant flexion angles: 10.6° at the set-up; 17.9° at the early backswing; 22.6° at the late backswing; 29.6° at the top of the backswing; and 8.4° at the end of the follow-through (Fig. 2A). The femur gradually flexed with the backswing and rapidly extended from the top of the backswing to the end of the follow-through. The implant rotation angles were 6.3° at the set-up, 7.4° at the early backswing, 8.1° at the late backswing, 13.0° at the top of the backswing, and 2.7° at the end of the follow-through (Fig. 2B). The femur exhibited progressive internal rotation with the backswing. More than 10° of the implant external rotation was recognized from the top of the backswing to the end of the follow-through.

Subjects undergoing TKA in the trail knee had the following implant flexion angles: 17.1 ± 20.4° (range, 4.3–40.6°) at the set-up position; 19.3 ± 20.3° (range, 6.7–42.8°) at the early backswing; 12.9 ± 8.6° (range, 9.1–22.8°) at the late backswing; 14.3 ± 8.1° (range, 9.8–23.6°) at the top of the backswing; and 29.9 ± 11.5° (range, 18.2–41.1°) at the end of the follow-through (Fig. 2A). The swing from the top of the backswing to the end of the follow-through produced the trail knee flexion. The implant rotation angles were −9.8 ± 7.7° (range, −4.2 to −18.5°) at the set-up, −12.5 ± 7.6° (range, −6.6 to −21.0°) at the early backswing, −13.9 ± 6.6° (range, −8.9 to −21.4°) at the late backswing, −16.0 ± 6.7° (range, −12.1 to −23.7°) at the top of the backswing, and 5.5 ± 4.9° (range, 0.1–9.7°) at the end of the follow-through (Fig. 2B). The femur exhibited progressive external rotation with the backswing (Fig. 3). More than 20° of the implant internal rotation was recognized from the top of the backswing to the end of the follow-through.

Stationary Cycling

The implant flexion angles were 100.0 ± 9.1° (range, 81.9–108.5°) at the top position of the crank, 91.8 ± 9.7° (range, 77.5–107.5°) at 25% phase, 74.2 ± 14.9° (range, 53.9–100.3°) at 50% phase, 51.7 ± 8.7° (range, 40.8–67.7°) at 75% phase, and 37.7 ± 9.6° (range, 17.3–46.7°) at the bottom position of the crank (Fig. 4A). The implant axial rotation angles were −8.1 ± 4.5° (range, −12.9 to 1.1°) at the top position, −6.6 ± 4.5° (range, −13.0 to 1.5°) at 25% phase, −5.2 ± 5.8° (range, −14.0 to 4.7°) at 50% phase, −3.4 ± 5.2° (range, −9.7 to 6.1°) at 75% phase, and

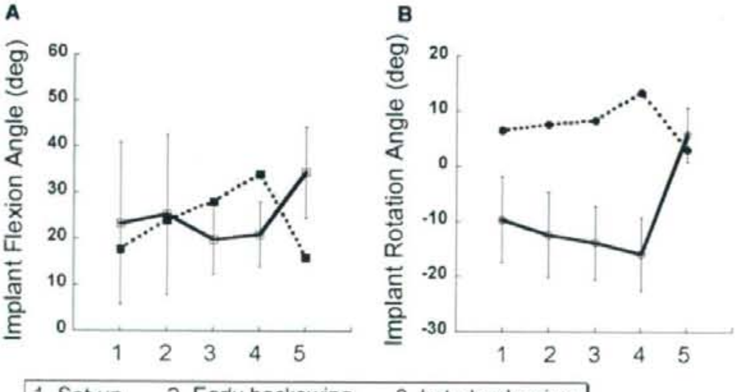

Figure 2. In vivo implant flexion (A) and rotational (B) angles for the golf swing: (1) set-up, (2) early backswing, (3) late backswing, (4) top of the backswing, and (5) end of the follow-through. The dotted line represents the lead (left) knee; the solid line represents the trail (right) knee. The positive or negative flexion value was defined as flexion or extension of the femoral component relative to the tibial component (A). The positive or negative rotation value was defined as internal or external rotation of the femoral component relative to the tibial component (B).

Figure 3. Examples of top views for a right-handed subject with a cruciate-retaining TKA in the trail (right) knee show axial rotation of the femoral component relative to the tibial component during the golf swing: (1) set-up, (2) early backswing, (3) late backswing, (4) top of the backswing, and (5) end of the follow-through. External rotation (overall about 8°) is gradually demonstrated from set-up (1) to the top of the backswing (4). More than 20° of internal rotation is rapidly demonstrated from the top of the backswing (4) to the end of the follow-through (5).

$-1.3 \pm 3.8°$ (range, -7.0 to $4.9°$) at the bottom position (Fig. 4B). The femur exhibited a normal rotational pattern with knee extension in all eight knees (Fig. 5).

The absolute value of the rotational motion from the top of the backswing to the end of the follow-through ($18.7 \pm 6.0°$; range, 10.3–23.8°) was significantly larger than during the stationary cycling from the top position to the bottom position ($6.7 \pm 2.6°$; range, 3.0–9.5°) ($p < 0.01$). No significant differences were found in the absolute values of the rotational motion between the backswing ($6.3 \pm 1.3°$ range, 5.2–7.9°) and the stationary cycling ($6.7 \pm 2.6°$ range, 3.0–9.5°) ($p = 0.73$).

DISCUSSION

Axial femorotibial rotation during flexion has been seen in previous in vivo kinematic analyses.[23–25] Stiehl et al. reported an average of 4.7° rotation in a flat on flat total condylar knee arthroplasty during deep knee bend.[23] In addition, Dennis et al. reported axial rotations in multiple TKA designs of 2.8° during deep knee bend.[24] We examined in vivo kinematics of TKA during golf swing and stationary cycling; the golf swing is a quite different from knee flexion–extension activities (e.g., stationary cycling, deep knee bend,[23–25] and step-up.[25]). The backswing produced progressive axial rotation, whereas the golf swing from the top of the backswing to the end of the follow-through rapidly produced high magnitudes of axial rotations (18.7° on average). In contrast, stationary cycling produced significantly less overall rotation than the golf swing from the top of the backswing to the end of the follow-through. During cycling, the axial rotations were 6.7° from the top of the crank to the bottom of the crank.

Excessive internal–external rotations lead to contact locations at the extreme edges of the tibial polyethylene surface.[27,28] Edge loading can cause chronic wear and fracture of the insert. Therefore, the high rotations when playing golf may be a concern with regard to long-term prognosis. Mallon and Callaghan reported that 16% of golfers with TKAs have a mild ache in the knee while playing and 35% have a mild ache after playing.[19] Furthermore, radiographic loosening among golfers with TKA was common in their study, occurring in 54% of all knees studied and 79% of cemented prostheses. The majority of members of the Knee Society suggested the use of a golf cart while playing, consistent with our opinion. Our findings suggest that golfers with a painful TKA should be encouraged to make half or three-quarter swings while also reducing the amount of golf that they play. The use of soft-spike golf shoes is also recommended to reduce the rotational torques on knee.[29,30]

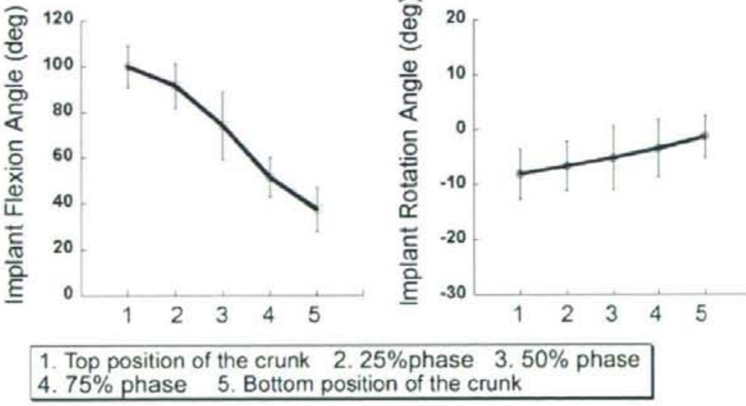

Figure 4. In vivo implant flexion (A) and rotational (B) angles from the top position of the crank to the bottom position of the crank: (1) top position, (2) 25% phase, (3) 50% phase, (4) 75% phase, and (5) bottom position. The positive or negative value of implant flexion was defined as flexion or extension of the femoral component relative to the tibial component (A). The positive or negative value of implant rotation was defined as the internal or external rotation of the femoral component relative to the tibial component (B).

Figure 5. Sequence of top views (3 frames per second) are shown for a subject with a left cruciate-retaining TKA, experiencing gradually internal rotation (overall about 9°) during stationary cycling: (1) top position of the crank, (2) 25% phase, (3) 50% phase, (4) 75% phase, and (5) bottom position of the crank.

The rotational motions from the top of the backswing to the end of the follow-through were greater in the trail knees than in the lead knee. However, the rotational torques and peak force are much greater on the lead knee.[20,31] The trail knee has its peak force at the end of the backswing when the club is moving slowly.[19,31] However, the lead knee has its peak force near impact and follow-through when most of the weight transfers to the lead knee.[31] The golf swing can produce a more stressful condition relative to the lead knee than the trail knee. Mallon et al. reported that right-handed golfers with left TKAs had significantly more pain while playing and after playing.[19] In our study, the lead knee demonstrated more than 10° of external rotation from the top of the backswing to the end of the follow-through.

During stationary cycling, axial rotation was within the ranges that the articulating surface geometries of the polyethylene inserts are designed to allow. The femur exhibited progressive internal rotation relative to the tibia with knee extension. Furthermore, riding a bicycle allows the individual to protect the knee from high impact forces. Ericson et al. used a knee model to predict tibiofemoral load of 1.2 times body weight during cycling in a normal subject.[32] D'Lima et al. measured in vivo knee forces of near one times body weight during stationary cycling after TKA.[33] To increase muscular strength and endurance with little risk for injuries, stationary cycling is a good recreational endurance exercise. Ericson et al. demonstrated the high magnitude of vastus medialis and lateralis activity during cycling.[34] Therefore, stationary cycling is generally recommended for patients with TKA who wish to remain physically active. Riding a bicycle is a popular activity for recreation and transportation. The stationary bike prevents injuries from falls.

During stationary cycling, the implant flexion angle was 100° in the maximally flexed position. McLeod et al. also described that about 100° of flexion is needed before a complete crank cycle can be performed.[22] Naturally, the femur exhibited progressive extension with pedaling from the top to the bottom of the crank. Each knee possessed characteristic patterns of knee flexion and rotation during golf swing, differences that can be explained by the skill level in golf. On the contrary, each knee possessed similar results of flexion and rotation during cycling. Stationary cycling is not a technically demanding sports activity even for inexperienced patients.

The number of patients who expect to return to sports for enjoyment and fitness after a TKA is increasing. Those patients who played sports preoperatively are especially motivated to return to sports activity.[4] Patients should not be unnecessarily discouraged from participating in low-impact sports in which they had participated preoperatively. However, patients should be instructed regarding sport-specific risks, namely, excessive rotational motions around the knee during a golf swing. Return to play after surgery should be avoided until the quadriceps and hamstring muscles have sufficiently recovered their preoperative strength. The overall frequency of the activity may also be important. The number of swings over a few hours of playing golf are less than the number of motion cycles generated during a few minutes of cycling. Furthermore, regular clinical and radiographic follow-up examinations of the TKA are required to diagnose and respond to any complications in a timely manner.

Our study has two drawbacks. First, we were certainly limited by the small number of patients in the golf swing analysis. Further investigations with comparisons between the lead and trail knees and between implant types are needed. However, our study revealed the kinematics of knee torsional activity that before had not received attention. Second, we were unable to collect data during the downswing because the flat panel detector provided only 3 frames per second; fluoroscopy is now commercially available with 30 frames per second that will capture the appropriate positions during highly dynamic activities. However, the flat panel detector was useful in capturing the dynamic activities because it has a greater field of view than fluoroscopy.

In summary, we demonstrated that unusual ranges of rotational motions occur at very high speeds during golf swing in comparison to stationary cycling. Our results suggest that edge loading induced by excessive internal–external rotation may be a concern with regard to the long-term prognosis following TKA. For stationary cycling, the femur exhibited progressive internal rotation relative to the tibia with knee extension within usual ranges of internal–external rotation. Generally, stationary cycling should thus be recommended to patients with TKA who wish to remain physically active.

ACKNOWLEDGMENTS

This study was supported by a grant from the Japan Sports Medicine Foundation, Inc.

REFERENCES

1. Colizza WA, Insall JN, Scuderi GR. 1995. The posterior stabilized total knee prosthesis. Assessment of polyethylene damage and osteolysis after a ten-year-minimum follow-up. J Bone Joint Surg [Am] 77:1713–1720.
2. Gill GS, Joshi AB. 2001. Long-term results of cemented, posterior cruciate ligament-retaining total knee arthroplasty in osteoarthritis. Am J Knee Surg 14:209–214.
3. Rodriguez JA, Bhende H, Ranawat CS. 2001. Total condylar knee replacement: A 20-year followup study. Clin Orthop 388: 10–17.
4. Bradbury N, Borton D, Spoo G, et al. 1998. Participation in sports after total knee replacement. Am J Sports Med 26:530–535.
5. Weiss JM, Noble PC, Conditt MA, et al. 2002. What functional activities are important to patients with knee replacements? Clin Orthop 404:172–188.
6. American College of Sports Medicine Position Stand. 1998. The recommended quantity and quality of exercise for developing and maintaining cardiorespiratory and muscular fitness, and flexibility in healthy adults. Med Sci Sports Exerc 30:975–991.
7. Howe TE, Rochester L, Jackson A, et al. 2007. Exercise for improving balance in older people. Cochrane Database Syst Rev 17:CD004963.
8. Williford HN, East JB, Smith FH, et al. 1986. Evaluation of warm-up for improvement in flexibility. Am J Sports Med 14:316–319.
9. Pollock ML, Dimmick J, Miller HS, et al. 1975. Effects of mode of training on cardiovascular function and body composition of adult men. Med Sci Sports Exerc 7:139–145.
10. Cooper KH, Pollock ML, Martin RP, et al. 1976. Physical fitness levels vs selected coronary risk factors. A cross-sectional study. JAMA 236:166–169.
11. Pescatello LS, Franklin BA, Fagard R, et al. 2004. American College of Sports Medicine position stand. Exercise and hypertension. Med Sci Sports Exerc 36:533–553.
12. Dubs L, Gschwend N, Munzinger U. 1983. Sport after total hip arthroplasty. Arch Orthop Trauma Surg 101:161– 169.
13. Christiansen C. 1995. Osteoporosis: diagnosis and management today and tomorrow. Bone 17:513S–516S.
14. Kuster MS. 2002. Exercise recommendations after total joint replacement: a review of the current literature and proposal of scientifically based guidelines. Sports Med 32:433–445.
15. Kilgus DJ, Dorey FJ, Finerman GA, et al. 1991. Patient activity, sports participation, and impact loading on the durability of cemented total hip replacements. Clin Orthop 269:25–31.
16. Schmalzried TP, Shepherd EF, Dorey FJ, et al. 2000. The John Charnley Award. Wear is a function of use, not time. Clin Orthop 381:36–46.
17. McGrory BJ, Stuart MJ, Sim FH. 1995. Participation in sports after hip and knee arthroplasty: review of literature and survey of surgeon preferences. Mayo Clin Proc 70:342–348.
18. Mallon WJ, Liebelt RA, Mason JB. 1996. Total joint replacement and golf. Clin Sports Med 15:179–190.
19. Mallon WJ, Callaghan JJ. 1993. Total knee arthroplasty in active golfers. J Arthroplasty 8:299–306.
20. Gatt CJ, Pavol MJ, Parker RD, et al. 1998. Three-dimensional knee joint kinetics during a golf swing. Influences of skill level and footwear. Am J Sports Med 26:285–294.
21. Ericson MO, Bratt A, Nisell R, et al. 1986. Load moments about the hip and knee joints during ergometer cycling. Scand J Rehabil Med 18:165–172.
22. McLeod WD, Blackburn TA. 1980. Biomechanics of knee rehabilitation with cycling. Am J Sports Med 8:175–180.
23. Stiehl JB, Komistek RD, Dennis DA. 1999. Detrimental kinematics of a flat on flat total condylar knee arthroplasty. Clin Orthop 365:139–148.
24. Dennis DA, Komistek RD, Mahfouz MR, et al. 2004. A multicenter analysis of axial femorotibial rotation after total knee arthroplasty. Clin Orthop 428:180–189.
25. Victor J, Banks S, Bellemans J. 2005. Kinematics of posterior cruciate ligament-retaining and -substituting total knee arthroplasty: a prospective randomised outcome study. J Bone Joint Surg [Br] 87:646–655.
26. Hamai S, Miura H, Higaki H, et al. 2008. Kinematic analysis of kneeling in cruciate-retaining and posterior-stabilized total knee arthroplasties. J Orthop Res 26:435–443.
27. Wasielewski RC, Galante JO, Leighty RM, et al. 1994. Wear patterns on retrieved polyethylene tibial inserts and their relationship to technical considerations during total knee arthroplasty. Clin Orthop 299:31–43.
28. Harman MK, Banks SA, Hodge WA. 2001. Polyethylene damage and knee kinematics after total knee arthroplasty. Clin Orthop 392:383–393.
29. McCarroll JR. 1996. The frequency of golf injuries. Clin Sports Med 15:1–7.
30. Guten GN. 1996. Knee injuries in golf. Clin Sports Med 15: 111–128.
31. Stover CN, Wiren G, Topaz SR. 1976. The modern golf swing and stress syndromes. Phys Sports Med 4:42–47.
32. Ericson M. 1986. On the biomechanics of cycling. A study of joint and muscle load during exercise on the bicycle ergometer. Scand J Rehabil Med Suppl 16:1–43.
33. D'Lima DD, Patil S, Steklov N, et al. 2005. The Chitranjan Ranawat Award: in vivo knee forces after total knee arthroplasty. Clin Orthop 440:45–49.
34. Ericson MO, Nisell R, Arborelius UP, et al. 1985. Muscular activity during ergometer cycling. Scand J Rehabil Med 17: 53–61.

The evaluation of post-operative alignment in total knee replacement using a CT-based navigation system

H. Mizu-uchi,
S. Matsuda,
H. Miura,
K. Okazaki,
Y. Akasaki,
Y. Iwamoto

From Kyushu University, Fukuoka, Japan

We compared the alignment of 39 total knee replacements implanted using the conventional alignment guide system with 37 implanted using a CT-based navigation system, performed by a single surgeon. The knees were evaluated using full-length weight-bearing anteroposterior radiographs, lateral radiographs and CT scans.

The mean hip-knee-ankle angle, coronal femoral component angle and coronal tibial component angle were 181.8° (174.2° to 188.3°), 88.5° (84.0° to 91.8°) and 89.7° (86.3° to 95.1°), respectively for the conventional group and 180.8° (178.2° to 185.1°), 89.3° (85.8° to 92.0°) and 89.9° (88.0° to 93.0°), respectively for the navigated group.

The mean sagittal femoral component angle was 85.5° (80.6° to 92.8°) for the conventional group and 89.6° (85.5° to 94.0°) for the navigated group.

The mean rotational femoral and tibial component angles were -0.7° (-8.8° to 9.8°) and -3.3° (-16.8° to 5.8°) for the conventional group and -0.6° (-3.5° to 3.0°) and 0.3° (-5.3° to 7.7°) for the navigated group.

The ideal angles of all alignments in the navigated group were obtained at significantly higher rates than in the conventional group. Our results demonstrated significant improvements in component positioning with a CT-based navigation system, especially with respect to rotational alignment.

Total knee replacement (TKR) has become one of the most successful procedures in orthopaedics with survival rates greater than 90% after 15 years.[1,2] The success of this procedure depends on many factors, including the pre-operative condition of the patient, the design and materials of the components and surgical techniques.[1-16] It is important to position the femoral and tibial components accurately and to balance the soft tissues. Malpositioning of the component can lead to failures due to aseptic loosening, instability, polyethylene wear and dislocation of the patella.[1-14]

Various surgical techniques and systems of instrumentation have been devised to obtain optimal post-operative alignment of the components. In the coronal plane it is recommended that the femoral and tibial components be positioned with less than 3° of error,[3,4] but such placement can only be achieved in 70% to 80% of patients using intra- or extramedullary alignment guides.[5,6] The point of entry of the intramedullary alignment guide is critical as it can change both the coronal and the sagittal alignment.[7] For rotational alignment of the femoral component, use of the Whiteside line and the transepicondylar axis is recommended to avoid problems with the patella.[8,9] However, the transepicondylar axis can be identified visually within 3° in only 75% of arthritic knees[17] and there may be errors in its identification when using a mini-invasive approach.[18] We cannot expect a high degree of accuracy using conventional techniques for rotational alignment by palpating anatomical landmarks.[17,19,20]

In order to improve post-operative alignment, navigation systems have been developed for TKR. Many clinical and experimental studies of these systems have shown that the accuracy of implanted components can be improved in spite of the increase in costs and operating time.[21-31] This may not, however, improve the outcome in the short-term.[32] Image-free navigation systems estimate the centre of the joint kinematically and digitise the anatomical landmarks. CT-based navigation systems allow three-dimensional pre-operative planning from the CT data and surface-matching registration. With both systems, over 90% of the operated knees achieved alignment of the mechanical axis of the leg within 3° of neutral,[21-26] but opinions differ as to the accuracy of image-free systems in

H. Mizu-uchi, MD, PhD, Orthopaedic Surgeon
S. Matsuda, MD, PhD, Assistant Professor, Orthopaedic Surgeon
H. Miura, MD, PhD, Associate Professor, Orthopaedic Surgeon
K. Okazaki, MD, PhD, Assistant Professor, Orthopaedic Surgeon
Y. Akasaki, MD, Orthopaedic Surgeon
Y. Iwamoto, MD, PhD, Professor, Chairman, Orthopaedic Surgeon
Department of Orthopaedic Surgery, Graduate School of Medical Sciences
Kyushu University, 3-1-1, Maidashi, Higashi-ku, Fukuoka City, Fukuoka, 812-8582, Japan.

Correspondence should be sent to Professor S. Matsuda; e-mail: mazda@ortho.med.kyushu-u.ac.jp

doi:10.1302/0301-620X.90B8.20265 $2.00

J Bone Joint Surg [Br] 2008;90-B:1025-31.
Received 27 September 2007; Accepted after revision 14 March 2008

Table I. The pre-operative demographic data for the conventional and the navigated groups

	Conventional group (39 knees)	Navigated group (37 knees)
Mean age in yrs (range)	76.9 (68 to 85)	75.4 (61 to 87)
Gender		
Male	8	8
Female	31	29
Diagnosis		
Osteoarthritis	36	35
Rheumatoid arthritis	3	2
Pre-operative KSS* (range)	54.8 (21 to 76)	54.4 (10 to 73)
Maximum extension (°) (range)	-5.5 (-30 to 0)	-11.9 (-40 to 0)
Maximum flexion (°) (range)	119.4 (80 to 150)	118.6 (85 to 145)
Pre-operative FTA† (°) (range)	183.8 (160.2 to 194.4)	181.6 (161.0 to 194.0)
Mean follow-up time in yrs (range)	2.3 (0.5 to 4.7)	1.8 (0.5 to 4.4)

* KSS, Knee society score

† FTA, femorotibial angle

obtaining rotational alignment.[22,24,27,28,33] Stockl et al[28] used the post-operative CT scan method and concluded that the image-free navigation systems achieved significantly better rotational alignment of the femoral component than did the conventional group. However, their range of alignment was relatively large (-7° to +4°). Siston et al[33] found that an image-free navigation system was no more accurate than four traditional techniques in establishing appropriate femoral rotation in ten cadaver specimens. Little information has been published on the rotational alignment of CT-based navigation systems. Registration in a CT-based navigation system uses surface matching of the large aspects of bones, whereas the image-free systems are required to specify anatomical landmarks accurately. We hypothesised that a CT-based system would improve both rotational and coronal alignment. The purpose of this study was to evaluate the accuracy of a CT-based navigation system for TKR in the coronal and rotational planes compared with the use of conventional alignment guides, when employed by a single surgeon.

Patients and Methods

Of a total of 137 primary TKRs performed in 119 patients by a single surgeon (SM) between January 2002 and January 2006, 81 knees in 68 patients had the Nexgen legacy posterior stabilised prosthesis (Zimmer, Warsaw, Indiana). A conventional alignment guide system and a CT-based navigation system were used in alternate patients. A study of these patients was approved by the Institutional Review Board, and they were informed of the risk of radiation exposure required. Of the 68 patients, informed consent was obtained from 63 (76 knees). A conventional alignment guide system was used in 39 knees in 32 patients (the 'conventional' group), and in 37 knees in 31 patients a CT-based navigation system was used (the 'navigated' group). After operation all patients in both groups were evaluated using full-length weight-bearing anteroposterior and lateral radiographs. All patients in the conventional group and 28 knees in 23 patients in the navigated group were assessed using CT scans. The Knee Society scoring system[34] was used to evaluate the pre-operative status of the knee one week before the surgery. The demographic data for both groups are presented in Table I; there was little difference between the two groups except for the angle of maximum extension.

Pre-operative planning procedures and surgical technique

The conventional group. Full-length weight-bearing anteroposterior radiographs were taken with the patella positioned at the centre of the femoral condyles. In the lateral films care was taken to ensure that the posterior condyles of the femur were not misaligned.

A standard medial parapatellar incision and approach was used. For the distal femur, the intramedullary alignment guide was inserted slightly medial to the midpoint of the femoral condyles. This entry point was determined as the position where the intramedullary line of the femoral canal exits the femoral condyles on the full-length anteroposterior radiographs. The distal femoral cutting block was then attached to the alignment guide and adjusted to the anatomical valgus angle of the femur (mean 5.9°, 3.0° to 9.0°). After cutting the distal femur, the cutting block was set to 3° of external rotation from the posterior condylar line. The appropriate cuts were then made.

The extramedullary alignment guide was used for cutting the proximal tibia and was set at a level approximately 10 mm distal to the lateral articular surface of the tibia. The sagittal alignment of the tibia was set parallel to the mechanical axis, and the posterior slope of the tibial component fixed in relation to the lateral tibial plateau.[35] The rotational alignment of the tibial component was adjusted to the anteroposterior axis between the centre of the cut

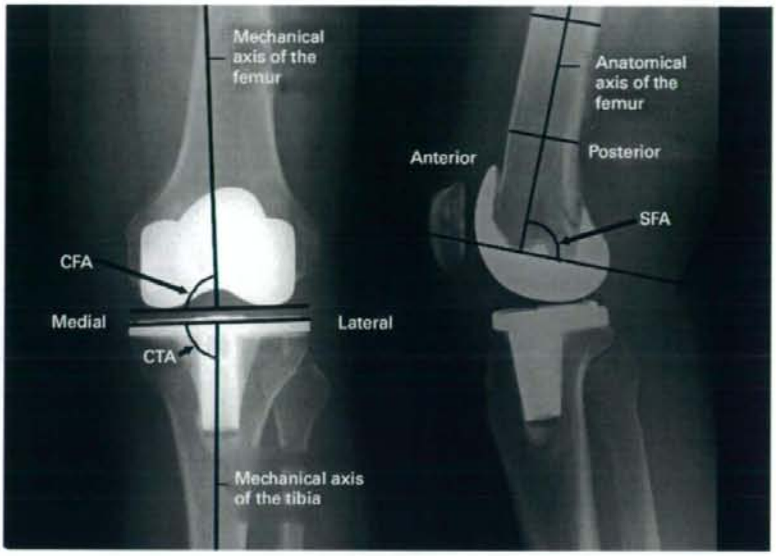

Fig. 1

Evaluation of the coronal and sagittal alignment of the components. The coronal femoral component angle (CFA) is the medial angle between the mechanical axis of the femur and the horizontal axis of the two prosthetic condyles. The coronal tibial component angle (CTA) is the medial angle between the mechanical axis of the tibia and the horizontal axis of the tibial tray. The sagittal femoral component angle (SFA) is the posterior angle between the anatomical axis of the femur and a tangent to the distal part of the femoral component.

surface and the border of the medial third of the tibial tuberosity.[36,37] This axis was chosen to avoid rotational mismatch of the femoral and tibial components, and to achieve better patellar tracking.[10] The patella was resurfaced in all patients. All the femoral, tibial and patellar components were fixed with cement.

The navigated group. We used a CT-based navigation system (Vector Vision Knee 1.5. Brain LAB Inc., Heimstetten, Germany). For the initial CT scans, a 100 mm section of the femoral head, a 200 mm section whose midpoint was the knee joint and a 100 mm section of the distal tibia were scanned with a slice thickness of 2 mm. The scanning time was approximately 10 seconds and the calculated radiation dose for the procedure was 3.7 mSV. The cost was approximately US$ 120 to 130. From these data, we defined the centre of the femoral head and the centre of the ankle joint after adjusting for the bone threshold and the window level and width. The bone threshold value was between 100 HU and 150 HU according to the patient's CT data; the extra artefact was deleted and the bone surface identified as clearly as possible. The femur, tibia and patella were then separated from each other at four points, namely the intercondylar eminence, the lateral tibial plateau, the medial tibial plateau, and the centre of the patella.

The anatomical axis of the femur was defined as the straight line between the centre of the intramedullary canal of the proximal and distal parts of the femur in both the coronal and sagittal planes. The mechanical axis of the femur was taken as the straight line between the centre of the head of the femur and the centre of the distal condyles. The coronal alignment of the femoral component was planned to be perpendicular to the mechanical axis of the femur and the sagittal alignment to be perpendicular to the anatomical axis of the distal femur in order to avoid notching of the femur due to the anterior bowing (mean 3.0°; 1.0° to 6.0°, in flexion to the mechanical axis). The rotational alignment was adjusted to the surgical epicondylar axis, which is a line connecting the sulcus of the medial epicondyle and the most prominent point of the lateral epicondyle of the femur.[8,9] After aligning the femoral component to the axis the size of the femoral component was adjusted as close as possible to the posterior condyles. The mechanical axis of the tibia was defined by a straight line between the centre of the cut of the proximal tibia and the centre of the ankle joint.[38] The planned coronal alignment of the tibial component was perpendicular to this axis. The planned sagittal alignment of the tibial component was parallel to the lateral tibial slope (mean 6.8°; 5.0° to 8.0°, to the mechanical axis).[35] The rotational alignment was adjusted to a line from the medial third of the tubercle at the level of the patellar tendon attachment to the centre of the cut surface of the tibia. The tibial component was positioned

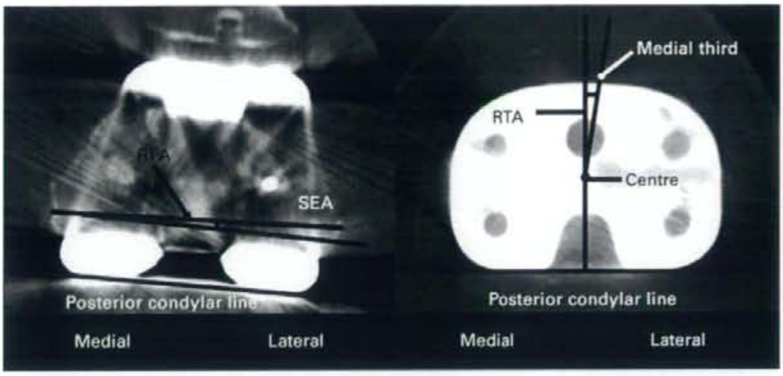

Fig. 2

Evaluation of the rotational alignment of the components. The rotational femoral component angle (RFA) is the angle between the surgical epicondylar axis (SEA) and the posterior condylar line of the femoral component. The rotational tibial component angle (RTA) is the angle between a line connecting the centre of the tibial component with the medial third of the tibial tubercle and the line perpendicular to the posterior condylar line of the tibial component.

Table II. Intra- and inter-observer reliability (κ values)

	Conventional group (39 knees)	Navigated group (37 knees)
Intra-observer reliability	0.94	0.95
Intra-observer reliability (observer A)	0.96	0.97
Intra-observer reliability (observer B)	0.96	0.97

10 mm distal from the highest point of the tibial plateau and a size was chosen so that the component would not overhang the medial border of the tibia. The pre-operative planning time was approximately 15 to 20 minutes.

At operation, the same medial parapatellar approach was used as in the conventional group. The reference clamp was fixed to the distal femur or the proximal tibia with one or two pins. Registration using surface matching of the bones was done with a pointer to match the corresponding three-dimensional CT images on the screen. A minimum of eight to a maximum of 20 points were registered until an accuracy of 1.9 mm or better was achieved. Using the cutting block adapter, the femoral and tibial blocks were positioned to match the plane of cut that had been determined before operation and was shown on the navigation system. After resection, all the planes were checked by the verification tool of the navigation system. The patella was resurfaced in all patients. All the femoral, tibial, and patellar components were fixed with cement.

Evaluation of post-operative alignment. The knees were assessed using the knee and functional score of the Knee Society scoring system six months after operation. Student's *t*-test was used to identify statistically significant differences ($p < 0.05$).

The alignment in the coronal plane was measured on the anteroposterior whole-leg radiograph (Fig. 1). The mechanical axis of the leg was defined as the hip-knee-ankle angle, which is the angle between the line connecting the centre of the hip with that of the knee, the mechanical axis of the femur, and the line connecting the centre of the knee with that of the ankle joint, which is the mechanical axis of the tibia. The ideal hip-knee-ankle angle was defined as within 3° of 180°. The coronal femoral component angle was measured as the medial angle between the mechanical axis of the femur and the horizontal axis of the two prosthetic condyles. The coronal tibial component angle was measured as the medial angle between the mechanical axis of the tibia and the horizontal axis of the tibial tray. Ideally, both these angles measured within 2° of 90°.

Alignment in the sagittal plane was measured on lateral radiographs (Fig. 1). The sagittal femoral component angle was defined as the posterior angle between the anatomical axis of the distal one-third of the femur and a tangent to the distal part of the femoral component. The tangent was

Table III. The differences of absolute value from the target angle (°)

	Target angle	Conventional group	Navigated group
Hip-knee-ankle angle (°; range)	180	2.7 (0 to 8.3)	1.4 (0 to 5.1)
Coronal femoral component angle (°; range)	90	2.2 (1 to 6.0)	1.3 (0 to 4.2)
Coronal tibial component angle (°; range)	90	1.5 (0.2 to 5.1)	1.1 (0 to 3.0)
Sagittal femoral component angle (°; range)	90	4.7 (0.7 to 9.4)	1.5 (0 to 4.6)
Rotational femoral component angle (°; range)	0	2.7 (0.1 to 9.8)	1.6 (0.4 to 3.5)
Rotational tibial component angle (°; range)	0	4.8 (0 to 16.8)	2.5 (0 to 7.7)

treated to be parallel to the bone-implant interface of the distal part of the femoral component. The ideal angle lay within 3° of 90°.

Rotational alignment was measured on the CT scan (Fig. 2). A 200 mm section whose midpoint was the knee joint only was scanned with a slice thickness of 2 mm. The rotational femoral component angle was defined as the angle between the surgical epicondylar axis and the posterior condylar line of the femoral component. The rotational tibial component angle was defined as the angle between a line connecting the centre of the tibial component and the medial third of the tibial tubercle and a line perpendicular to the posterior condylar line of the tibial component. The ideal femoral component and rotational tibial angles are defined as within 3° of the target angle (0°).[17,27]

Statistical analysis. A Mann-Whitney U test was used to determine statistically significant differences ($p < 0.05$) in absolute value from the target angles between the two systems using these parameters. Fisher's exact probability test was used to compare the quality of implantation, measured against the ideal position, between the two systems with these parameters ($p < 0.05$). In addition, we evaluated a correlation between error in rotational alignment and the functional score for both groups using Spearman's correlation coefficient by rank test ($p < 0.05$). All measurements were done by two observers (HM and YA). The blinded data did not include the patient information and were numbered randomly. The mean values of three measurements using a digital X-ray measuring system (X-caliper; Eisenlohr Technologies Inc., Davis, California) were measured. The chance-corrected κ-coefficient was calculated to determine intra- and inter-observer agreement, with κ values interpreted according to the recommendations of Landis and Koch.[39] Intra- and interobserver reliability were almost perfect ($p < 0.001$ in each case, Table II).

Results

The mean post-operative Knee Society score was 94.9 (62 to 100) for the conventional and 95.0 (70 to 100) for the navigated group. The mean post-operative functional score was 78.1 (5 to 100) for the conventional group and 78.2 (30 to 100) for the navigated group. No significant difference was detected in these values for the two groups. No patients had a flexion contracture of more than 20° or a flexion angle of less than 90° at six months after surgery.

For coronal alignment, the mean hip-knee-ankle angle was 181.8° (174.2° to 188.3°) for the conventional and 180.8° (178.2° to 185.1°) for the navigated group. The mean coronal femoral component angle was 88.5° (84.0° to 91.8°) for the conventional and 89.3° (85.8° to 92.0°) for the navigated group. The mean coronal tibial component angle was 89.7° (86.3° to 95.1°) for the conventional and 89.9° (88.0° to 93.0°) for the navigated group. The differences in absolute value from the target angle are shown in Table III. There were significant differences in the absolute values from the target angle in tests for the hip-knee-ankle angle ($p < 0.01$) and the coronal femoral component angle ($p = 0.02$), but no significant difference in the coronal tibial component angle ($p = 0.24$) between the two groups. Ideal hip-knee-ankle, coronal femoral component, and coronal tibial component angles were obtained in 71.8% (28 of 39 knees), 71.8% (28 of 39 knees), and 76.9% (30 of 39 knees) of operations for the conventional group, and 91.9% (34 of 37 knees), 91.9% (34 of 37 knees), and 94.6% (35 of 37 knees) of operations for the navigated group ($p < 0.05$, $p < 0.05$, $p < 0.05$), respectively.

For sagittal alignment, the mean sagittal femoral component angle was 85.5° (80.6° to 92.8°) for the conventional and 89.6° (85.4° to 94.0°) for the navigated group. There was a significant difference in the absolute values from the target angle of the sagittal femoral component angle ($p < 0.0001$) between the two groups. Ideal sagittal femoral component angles were obtained in 43.6% (17 of 39 knees) in the conventional group and 89.2% (33 of 37 knees) in the navigated group ($p < 0.01$).

For rotational alignment, the mean rotational femoral component angle was -0.7° (-8.8° to 9.8°) for the conventional and -0.6° (-3.5° to 3.0°) for the navigated group. The mean rotational tibial component angle was -3.3° (-16.8° to 5.8°) for the conventional and 0.3° (-5.3° to 7.7°) for the navigated group. There was a significant difference in the absolute values from the target angle of the rotational femoral component ($p = 0.04$) and rotational tibial component angles ($p = 0.03$) between the two groups. Ideal rotational femoral component and rotational tibial component angles were obtained in 66.7% (26 of 39 knees) and 46.2% (18 of 39 knees) in the conventional group and 89.3% (25 of 28 knees) and 78.6% (22 of 28 knees) in the navigated group ($p = 0.04$ and 0.01), respectively. There was no significant correlation between errors in rotational alignment and the functional score for both the femoral and the tibial components.

Discussion

Total knee replacement has become a very successful procedure owing to improvements in prostheses and in surgical techniques. However, malpositioning of the components may occur when the conventional method is used.[1-14] Long-leg standing radiographs are commonly used for pre-operative planning, but they can be affected by the position of the limb and the direction of scanning because they are two-dimensional images. Other possible causes of error include bowing of the bones, severe deformities and obesity.

Navigation systems for TKR have been developed to reduce these errors. This study compared post-operative alignment achieved using CT-based navigation with that using the conventional system. For coronal alignment, the positioning of components was improved by the navigation system, with results similar to those of Nizard et al[25] and Perlick et al.[26] The CT-based system ensures the accuracy of positioning the components in the coronal plane.

The sagittal alignment of the components was improved by the navigation system. Poorer results with the conventional method seem to relate to the use of the intramedullary guide whose alignment is affected by its point of entry and direction. Mihalko et al[7] found differences in alignment in the sagittal plane using three different entry points for the intramedullary guide. Their trials on seven cadaver limbs varied between 2.2° of extension and 3.8° of flexion relative to the mechanical axis. With the image-free navigation system, many authors have concluded that this method is useful for cutting the distal femur perpendicular to the mechanical axis of the femur.[28] However, this method may increase the risk of notching the anterior cortex of the distal femur and require manual adjustment of the position of the cutting guide to avoid this. We chose the anatomical axis of the distal femur as the planned sagittal alignment of the femoral component to avoid notching. Post-operative sagittal alignment was also measured using the distal anatomical axis as a reference line to minimise the effect of sagittal bowing of the femur.

Few studies have yet demonstrated any advantages of the CT-based navigation system with respect to rotational alignment. In our series, 89.3% of the femoral components were implanted within 3° of the ideal rotational alignment and the range (-3.5° to 3.0°) was relatively small. Using the image-free system, it is uncertain whether digitising the bony landmarks is precise, and the accuracy of the rotational alignment is still uncertain.[22,24,27,28,33] Many authors[17,19,20] have reported variability in the identification of the transepicondylar axis. Yau et[19] found that the maximum combined error was 8.2°, with 5.3° at the medial femoral epicondyle and 2.9° at the lateral in the transepicondylar axis. These results suggest that surgeons are not able to rely completely on the accuracy of the image-free navigation system. Image-free systems are more widely used than the CT-based system, probably because of the need for pre-operative CT scans and the planning time.

Although this study has shown that the CT-based navigation system significantly improved the accuracy of the rotational alignment of the tibial component, the variation from the ideal angle of tibial alignment was larger than that of the femoral alignment, as others have noted.[22,24,27] One reason for this is the difficulty in determining the medial third of the tibial tubercle at the same point as was defined pre-operatively. Even so, 78.6% of the tibial components in the navigated group were implanted within 3° of the ideal rotational alignment, as has been found using an image-free navigation system.[22]

It is difficult to determine the ideal tibial rotational alignment because the method of defining the anteroposterior axis of the tibia is variable.[36,37] We used the line connecting the centre of the tibia and the medial third of the tibial tubercle as the reference axis to avoid the rotational mismatch between the femoral and tibial components[36,37] and to achieve better patellar tracking.[10]

Determining the indicator of 'outliers' is another difficult issue in tibial rotational alignment. Rotator restraint produced by the tibiofemoral linkage of the posterior stabilised design should be considered. However, the Nexgen legacy posterior stabilised prosthesis (Zimmer) has 12° of freedom of internal and external rotation in full extension. In this study, within 3° was chosen for the ideal range in order to be able to compare the accuracy with other navigation systems.[27]

Some reports[21,29] comparing the accuracy of the CT-based navigation system to that of the image-free navigation system show no differences in the accuracy of the post-operative alignment using the radiographs. Image-free navigation systems are widely used for computer-assisted surgery. Jenny et al[23] reported that 92.3% (217 of 235 knees) of operations had a coronal mechanical femorotibial angle within a range of ± 3° using the OrthoPilot system (Aesculap, Tuttlingen, Germany), compared with 72.3% (170 of 235 knees) with conventional methods. Tingart et al[30] reported that 94.8% (474 of 500 knees) of operations had a varus/valgus alignment within a range of ± 3° of 180° (the target angle of the mechanical axis) using the Vector-Vision CT-free Knee (BrainLAB, Munich, Germany; CI System Orthopedics, Munich, Germany), compared with 74.4% (372 of 500 knees) with conventional methods. The main disadvantage of the CT-based navigation system is that it requires pre-operative preparation with additional costs and exposure to radiation. However, our results show that the CT-based system has advantages over the image-free system, in particular in determining femoral rotation.

The current study has some limitations. The number of patients is relatively small. The post-operative alignment was evaluated by radiographs and/or CT images. This is a two-dimensional evaluation and is affected by the positioning of the limb and the direction of scanning, despite the fact that pre-operative planning and intra-operative procedures are performed in three dimensions. Cobb et al[40] reported the accuracy of unicompartmental knee replacement three-dimensionally from the pre-operative and post-operative CT images. It is important to evaluate the post-operative alignment three-dimensionally. However, our post-operative CT was performed only around the knee joint, in order to minimise the dose of radiation, and whole-leg alignment was evaluated by this method. The sagittal alignment of the tibial component was not evaluated as it was adjusted to the lateral anatomical tibial slope.

This study evaluated the accuracy of a CT-based navigation system using post-operative radiographs and CT scans. Our results demonstrate significant improvements in positioning of the components with the CT-based system, especially with respect to rotational alignment.

The authors wish to thank S Hamai, and S Fukagawa, Department of Orthopaedic Surgery Graduate School of Medical Sciences, Kyushu University, Fukuoka, Japan, for help in the blinded post-operative assessment.

No benefits in any form have been received or will be received from a commercial party related directly or indirectly to the subject of this article.

References

1. **Rodricks DJ, Patil S, Pulido P, Colwell CW Jr.** Press-fit condylar design total knee arthroplasty: fourteen to seventeen-year follow-up. *J Bone Joint Surg [Am]* 2007;89-A:89-95.
2. **Vessely MB, Whaley AL, Harmsen WS, Schleck CD, Berry DJ.** Long-term survivorship and failure modes of 1000 cemented condylar total knee arthroplasties. *Clin Orthop* 2006;452:28-34.
3. **Jeffery RS, Morris RW, Denham RA.** Coronal alignment after total knee replacement. *J Bone Joint Surg [Br]* 1991;73-B:709-14.
4. **Rand JA, Coventry MB.** Ten-year evaluation of geometric total knee arthroplasty. *Clin Orthop* 1988;232:168-73.
5. **Mahaluxmivala J, Bankes MJ, Nicolai P, Aldam CH, Allen PW.** The effect of surgeon experience on component positioning in 673 Press Fit Condylar posterior cruciate-sacrificing total knee arthroplasties. *J Arthroplasty* 2001;16:635-40.
6. **Petersen TL, Engh GA.** Radiographic assessment of knee alignment after total knee arthroplasty. *J Arthroplasty* 1988;3:67-72.
7. **Mihalko WM, Boyle J, Clark LD, Krackow KA.** The variability of intramedullary alignment of the femoral component during total knee arthroplasty. *J Arthroplasty* 2005;20:25-8.
8. **Berger RA, Rubash HE, Seel MJ, Thompson WH, Crossett LS.** Determining the rotational alignment of the femoral component in total knee arthroplasty using the epicondylar axis. *Clin Orthop* 1993;286:40-7.
9. **Matsuda S, Miura H, Nagamine R, et al.** A comparison of rotational landmarks in the distal femur and the tibial shaft. *Clin Orthop* 2003;414:183-8.
10. **Berger RA, Crossett LS, Jacobs JJ, Rubash HE.** Malrotation causing patellofemoral complications after total knee arthroplasty. *Clin Orthop* 1998;356:144-53.
11. **D'Lima DJ, Patil S, Steklov N, Colwell CW Jr.** Dynamic intraoperative ligament balancing for total knee arthroplasty. *Clin Orthop* 2007;463:208-12.
12. **Griffin WL, Fehring TK, Pomeroy DL, Gruen TA, Murphy JA.** Sterilization and wear-related failure in first- and second-generation press-fit condylar total knee arthroplasty. *Clin Orthop* 2007;464:16-20.
13. **Noble PC, Conditt MA, Cook KF, Mathis KB.** Patient expectations affect satisfaction with total knee arthroplasty. *Clin Orthop* 2006;452:35-43.
14. **Walker PS, Yildirim G, Sussman-Fort J, et al.** Factors affecting the impingement angle of fixed- and mobile-bearing total knee replacements: a laboratory study. *J Arthroplasty* 2007;22:745-52.
15. **Epinette JA, Manley MT.** Hydroxyapatite-coated total knee replacement: clinical experience at 10 to 15 years. *J Bone Joint Surg [Br]* 2007;89-B:34-8.
16. **Tai CC, Cross MJ.** Five- to 12-year follow-up of a hydroxyapatite-coated cementless total knee replacement in young, active patients. *J Bone Joint Surg [Br]* 2006;88-B:1158-63.
17. **Kinzel V, Ledger M, Shakespeare D.** Can the epicondylar axis be defined accurately in total knee arthroplasty? *Knee* 2005;12:293-6.
18. **Yau WP, Leung A, Liu KG, et al.** Errors in the identification of the transepicondylar and anteroposterior axes of the distal femur in total knee replacement using minimally-invasive and conventional approaches: a cadaver study. *J Bone Joint Surg [Br]* 2008;90-B:520-6.
19. **Yau WP, Leung A, Chiu KY, Tang WM, Ng TP.** Intraobserver errors in obtaining visually selected anatomic landmarks during registration process in non image-based navigation-assisted total knee arthroplasty: a cadaveric experiment. *J Arthroplasty* 2005;20:591-601.
20. **Jenny JY, Boeri C.** Low reproducibility of the intra-operative measurement of the transepicondylar axis during total knee replacement. *Acta Orthop Scand* 2004;75:74-7.
21. **Bathis H, Perlick L, Tingart M, et al.** Radiological results of image-based and non-image-based computer-assisted total knee arthroplasty. *Int Orthop* 2004;28:87-90.
22. **Chauhan SK, Scott RG, Breidahl W, Beaver RJ.** Computer-assisted knee arthroplasty versus a conventional jig-based technique: a randomised, prospective trial. *J Bone Joint Surg [Br]* 2004;86-B:372-7.
23. **Jenny JY, Clemens U, Kohler S, et al.** Consistency of implantation of a total knee arthroplasty with a non-image-based navigation system: a case-control study of 235 cases compared with 235 conventionally implanted prostheses. *J Arthroplasty* 2005;20:832-9.
24. **Matziolis G, Krocker D, Weiss U, Tohtz S, Perka C.** A prospective, randomized study of computer-assisted and conventional total knee arthroplasty: three-dimensional evaluation of implant alignment and rotation. *J Bone Joint Surg [Am]* 2007;89-A:236-43.
25. **Nizard RS, Porcher R, Ravaud P, et al.** Use of the Cusum technique for evaluation of a CT-based navigation system for total knee replacement. *Clin Orthop* 2004;425:180-8.
26. **Perlick L, Bathis H, Tingart M, Perlick C, Grifka J.** Navigation in total-knee arthroplasty: CT-based implantation compared with the conventional technique. *Acta Orthop Scand* 2004;75:464-70.
27. **Kim YH, Kim JS, Yoon SH.** Alignment and orientation of the components in total knee replacement with and without navigation support: a prospective, randomised study. *J Bone Joint Surg [Br]* 2007;89-B:471-6.
28. **Stockl B, Nogler M, Rosiek R, et al.** Navigation improves accuracy of rotational alignment in total knee arthroplasty. *Clin Orthop* 2004;426:180-6.
29. **Martin A, von Strempel A.** Two-year outcomes of computed tomography-based and computed tomography free navigation for total knee arthroplasties. *Clin Orthop* 2006;449:275-82.
30. **Tingart M, Luring C, Bathis H, et al.** Computer-assisted total knee arthroplasty versus the conventional technique: how precise is navigation in clinical routine? *Knee Surg Sports Traumatol Arthrosc* 2008;16:44-50.
31. **Nabeyama R, Matsuda S, Miura H, et al.** The accuracy of image-guided knee replacement based on computed tomography. *J Bone Joint Surg [Br]* 2004;86-B:366-71.
32. **Spencer JM, Chauhan SK, Sloan K, Taylor A, Beaver RJ.** Computer-navigation versus conventional total knee replacement: no difference in functional results at two years. *J Bone Joint Surg [Br]* 2007;89-B:477-80.
33. **Siston RA, Patel JJ, Goodman SB, Delp SL, Giori NJ.** The variability of femoral rotational alignment in total knee arthroplasty. *J Bone Joint Surg [Am]* 2005;87-A:2276-80.
34. **Insall JN, Dorr LD, Scott RD, Scott WN.** Rationale of the Knee Society clinical rating system. *Clin Orthop* 1989;248:13-14.
35. **Kuwano T, Urabe K, Miura H, et al.** Importance of the lateral anatomic tibial slope as a guide to the tibial cut in total knee arthroplasty in Japanese patients. *J Orthop Sci* 2005;10:42-7.
36. **Matsui Y, Kadoya Y, Uehara K, Kobayashi A, Takaoka K.** Rotational deformity in varus osteoarthritis of the knee: analysis with computed tomography. *Clin Orthop* 2005;433:147-51.
37. **Mizu-uchi H, Matsuda S, Miura H, et al.** The effect of ankle rotation on cutting of the tibia in total knee arthroplasty. *J Bone Joint Surg [Am]* 2006;88-A:2632-6.
38. **Matsuda S, Mizu-uchi H, Miura H, et al.** Tibial shaft axis does not always serve as a correct coronal landmark in total knee arthroplasty for varus knees. *J Arthroplasty* 2003;18:56-62.
39. **Landis JR, Koch GG.** The measurement of observer agreement for categorical data. *Biometrics* 1977;33:159-74.
40. **Cobb J, Henckel J, Gomes P, et al.** Hands-on robotic unicompartmental knee replacement: a prospective, randomised controlled study of the acrobot system. *J Bone Joint Surg [Br]* 2006;88-B:188-97.

Dynamic Activity Dependence of In Vivo Normal Knee Kinematics

Taka-aki Moro-oka,[1,2] Satoshi Hamai,[2] Hiromasa Miura,[2] Takeshi Shimoto,[3] Hidehiko Higaki,[3] Benjamin J. Fregly,[1] Yukihide Iwamoto,[2] Scott A. Banks[1,4]

[1]Department of Mechanical and Aerospace Engineering, University of Florida, 318 MAE-A, Mail Stop 116250, Gainesville, Florida 32611

[2]Department of Orthopaedic Surgery, Graduate School of Medical Sciences, Kyushu University, Fukuoka, Japan

[3]Department of Mechanical Engineering, Faculty of Engineering, Kyushu Sangyo University, Fukuoka, Japan

[4]The BioMotion Foundation, Palm Beach, Florida

Received 20 November 2006; accepted 25 January 2007

Published online in Wiley InterScience (www.interscience.wiley.com). DOI 10.1002/jor.20488

ABSTRACT: Dynamic knee kinematics were analyzed for normal knees in three activities, including two different types of maximum knee flexion. Continuous X-ray images of kneel, squat, and stair climb motions were taken using a large flat panel detector. CT-derived bone models were used for model registration-based 3D kinematic measurement. Three-dimensional joint kinematics and contact locations were determined using three methods: bone-fixed coordinate systems, interrogation of CT-based bone model surfaces, and interrogation of MR-based articular cartilage model surfaces. The femur exhibited gradual external rotation throughout the flexion range. Tibiofemoral contact exhibited external rotation, with contact locations translating posterior while maintaining 15° to 20° external rotation from 20° to 80° of flexion. From 80° to maximum flexion, contact locations showed a medial pivot pattern. Kinematics based on bone-fixed coordinate systems differed from kinematics based on interrogation of CT and MR surfaces. Knee kinematics varied significantly by activity, especially in deep flexion. No posterior subluxation occurred for either femoral condyle in maximum knee flexion. Normal knees accommodate a range of motions during various activities while maintaining geometric joint congruency. © 2007 Orthopaedic Research Society. Published by Wiley Periodicals, Inc. J Orthop Res 26:428–434, 2008

Keywords: tibiofemoral joint; kinematics; dynamic activity; flat panel detector; 3D/2D model registration; tibiofemoral contact

INTRODUCTION

3D-to-2D model registration techniques have been used to measure normal in vivo knee kinematics from radiographic images. These studies have provided clinically insightful information and spurred further complementary investigations. Research topics of current interest include exploration of knee kinematics over the full flexion range and development of techniques for generating and reporting data to provide enhanced physiologic insight.

3D kinematics studies have focused on motion from 0° to 90° of flexion. Asano et al.[1] reported a medial pivot motion pattern during static weight bearing from 0° to 90°. Komistek et al.[2] reported dynamic normal knee kinematics using shape-matching techniques with computed tomography (CT)-derived bone models. They showed that the lateral condyle experienced significantly more AP translation in activities up to 90° of flexion with no significant differences among activities. More recently, Li et al.[3] reported cartilage contact kinematics from 0° to 90° using bi-plane fluoroscopy and MRI-derived bone models. No study has analyzed dynamic, weight-bearing tibiofemoral motion from extension to maximum knee flexion.

3D knee kinematic studies also have used a variety of coordinate systems and joint contact computations to describe findings, making it sometimes difficult to compare results of one study to another. For example, varus–valgus motion determined from coordinate systems embedded in the bones can be interpreted to indicate separation of the joint surfaces. However, when the different sagittal slopes of the medial and lateral tibial surfaces are considered, varus–valgus motion can result from the condyles moving AP while remaining in contact with these surfaces. A complete

Correspondence to: Scott A. Banks (Telephone: 352-392-6109; Fax: 352-392-7303; E-mail: banks@ufl.edu)

mapping of joint surface separations provides a coordinate system-independent measure of articular apposition that avoids misinterpretation. To date, CT-derived bone models (CT model) have been primarily used for model registration-based kinematic measurements.[1,2,4] Determination of tibiofemoral contact conditions from CT models assumes uniform cartilage thickness. MR-based surface models including cartilage are superior for computing surface interactions, but suffer from less accurate bone definition, which can lead to less precise kinematic measurements.[5] The optimal approach, therefore, might be to perform model registration using CT-derived bone models with surface interrogations performed using MR-derived articular surfaces.

The purpose of this study was to analyze healthy knee kinematics in three activities from extension to maximum knee flexion using high-resolution dynamic flat-panel detector images. A secondary purpose was to consider cartilage thickness in tibiofemoral contact analysis and to compare different methods for reporting articular kinematics.

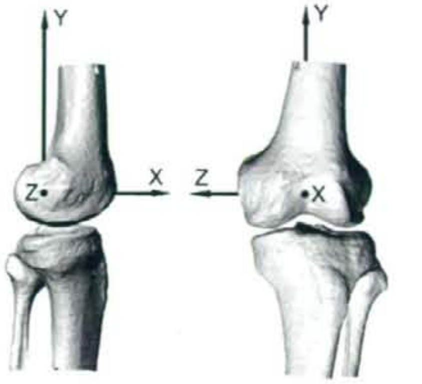

Figure 1. The mediolateral (Z) axis of both the femur and tibia/fibula was defined by fitting a cylinder to the posterior condyles of the femur. The mid point of the cylindrical axis was defined as the coordinate system origin for both tibia and femur.

MATERIALS AND METHODS

Six healthy male subjects, averaging 29 years (28–31), 171 cm (165–177), and 69 kg (55–80) gave informed consent to participate in this study as approved by the institutional review board. Bone models of the femur and tibia/fibula were created from CT (Toshiba, Aquilion, Tochigi, Japan) and MR (Hitachi, Airis II Comfort, Tokyo) scans of one leg. CT scans used a 512×512 image matrix, a 0.35×0.35 pixel dim, and a 1-mm thickness spanning approximately 150 mm above and below the joint line of the knee, and 2 mm slices through the centers of the hip and ankle. MR scans used a 512×512 image matrix, a 0.39×0.39 pixel dim, and a 1-mm thickness spanning more than 80 mm above and below the joint line of the knee. Scan time of MR ranged from 11 to 15 min. Exterior cortical bone edges for CT and external edges of both cortical bone and cartilage for MRI were segmented using commercial software (SliceOmatic, Tomovision, Montreal, CA), and these point clouds were converted into polygonal surface models (Geomagic Studio, Raindrop Geomagic, Research Triangle Park, NC). Anatomic coordinate systems were embedded in each bone model following conventions of previous studies.[5] The coordinate systems were first defined for the CT models. The mediolateral (Z) axis of both the femur and tibia/fibula was defined by fitting a cylinder to each posterior condyle of the femur (Fig. 1). The mid point of the cylindrical axis was defined as the coordinate system origin. The proximal/distal (Y) axis for the femur was defined by a line perpendicular to the cylindrical axis in the plane intersecting the femoral head center. The proximal/distal (Y) axis for the shank was perpendicular to the cylindrical axis in the plane intersecting the ankle center. The anteroposterior (X) axis was formed from the cross product of the first two. Next, the MR model was registered with the corresponding CT model in its initial reference pose in order to align the embedded coordinate systems in each bone model. Proprietary automated alignment software was used to match 3D bone surfaces (Geomagic Studio). Reported accuracy for this technique is less than 0.1 micrometers in length and 0.1 arcseconds in angle compared to a reference standard value.

Continuous sagittal X-ray images of kneel, squat, and stair-climb activities for each subject were taken using a flat panel detector (Hitachi, Clavis, 3 frames/s, image area 397×298 mm, 0.20×0.20 mm/pixel resolution) (Fig. 2). For the kneel activity, subjects placed their leg on a box, with the foot and ankle hanging freely, and applied their body weight to achieve maximum knee flexion. For the squat activity, the subject stood on a wheeled cart, moved rearward at >2.5 cm/s, so their knee position could be maintained in front of the flat-panel detector as they flexed from full extension to full flexion. For the stair activity, subjects ascended a two-step staircase in a reciprocal manner with knee motions recorded on the first step. A total of 293 images were used: 90 images for kneel, 130 for squat, and 73 for stair.

The 3D position and orientation of the tibia/fibula and femur were determined using previously reported shape matching techniques[4–6] (Fig. 3). A region of the flat-panel X-ray image was extracted and scaled to 512×512 square pixels for 3D shape registration. The CT models were projected onto the X-ray image and manually aligned with the bone projections. An automated matching algorithm using nonlinear least squares optimization, and an image edge-to-model edge distance criteria was used to refine registration of the bone models. RMS errors for this method were 0.53 mm for in-plane

Figure 2. Subjects performed kneeling (left), lunge (middle) and stair (right) activities while their knee motion was observed using a large flat panel x-ray image detector. The images show a left knee being studied. Kneeling was performed from 90° to maximum comfortable flexion. Squatting was performed from a standing position to maximum comfortable flexion. The stair activity captured the ascent phase from approximately 70° to 10° flexion.

translation, 1.6 mm for out-of-plane translation, and 0.54° for rotations in a previous study.[5] Propagation of these uncertainties to the articular surfaces results in a 95% confidence interval >2 mm for declaring separation of the femoral condyles from the tibial surface.

The kinematics of the joint were determined from the 3D position of each bone model using Cardan angles as described by Tupling and Pierrynowski.[7] Knee rotations were analyzed as a function of flexion angle. Spline interpolation with 5° flexion increments was used to create average kinematics for the group. The stair climb proceeded from flexion to extension; the kneel and squat proceeded from extension to flexion. Each subject began and completed each activity at slightly different flexion angles, so averages are reported for flexion angles from three to six knees. One-way ANOVA and post hoc tests (Bonferroni/Dunn) ($p < 0.05$) were used to examine differences among overall results.

The surface of each CT-derived tibial model was divided into medial and lateral compartments and represented as a cloud of points. For every image, a surface separation map was created by computing the minimum distance between each point on the tibial surface and all points on the femoral surface (Fig. 4). Medial and lateral condylar contact locations were computed as the geometric centroid of the region having <6 mm separation, which acknowledges uncertainty about cartilage thickness,[8,9] cartilage deformation, and measurement errors. The choice of separation threshold had a negligible effect on centroid location for thresholds above 3 mm. The angle between the kinematics of the femur with respect to the tibia.

Interactions of cartilage surfaces were determined from the MR-derived models. The bony part of the MR models was registered with the corresponding CT models using automated alignment software (Geomagic Studio). Knee kinematics determined from CT model registration were then used to orient the cartilage surfaces. Contact points were defined in the same manner for the MR models, except a 2-mm maximum separation threshold was used to define the region of contact, contact centroids, and rotational kinematics (Fig. 4).

RESULTS

Bony kinematics varied among activities. Femoral rotation during squatting was significantly different from kneeling at all flexion angles and differed from stair climbing from 25° to 35° flexion (Fig. 5A). However, the femur rotated externally with flexion in all three activities. Sharp external rotation was seen from 0° to 15° in squatting,

Figure 3. 3D-to-2D CT model-to-flat panel image registration was used to determine the kinematics of healthy knees during three weight bearing activities.

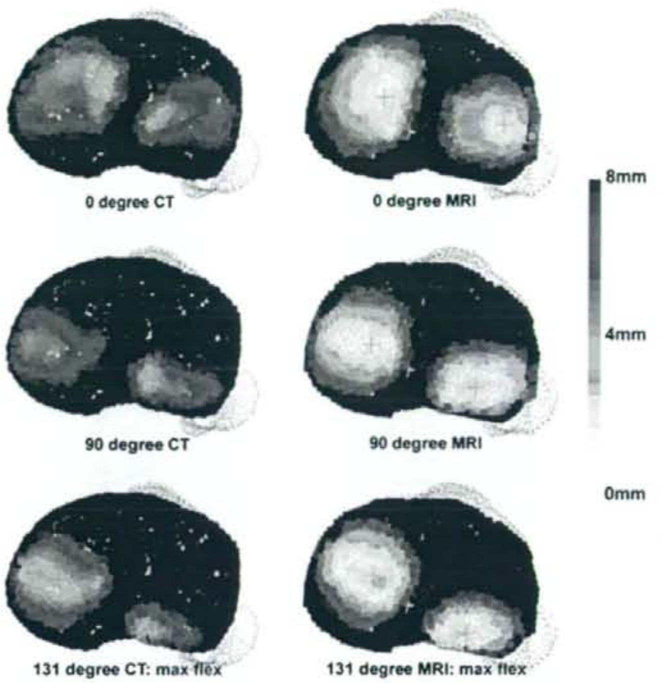

Figure 4. Separation distance mapping for squat at 0°, 90°, and maximum flexion (131°) in one subject. Pictures calculated from the MRI model and CT model are shown at the same flexion angle. The centroids of the contact areas are shown as a red cross to indicate the estimated contact location. The picture shows irregular estimated contact regions based on the CT derived models, while the MR derived models of articular cartilage show uniformly rounded contact region estimates

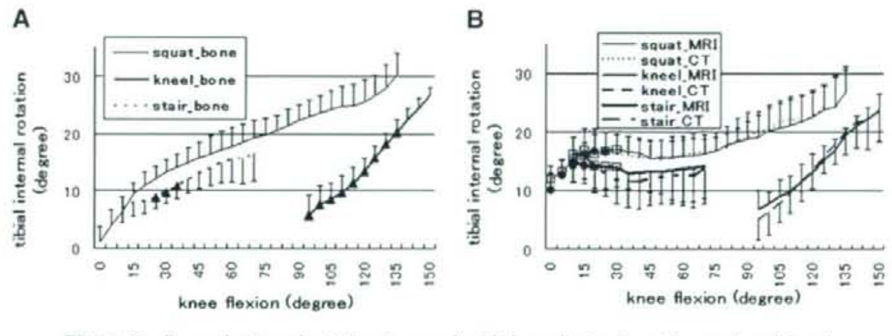

Figure 5. Femoral external rotation increased with knee flexion for stair, squat and kneel activities. A: Femoral external rotations based on bone-embedded coordinate systems. Solid triangles on the stair and kneel represent statistically significant differences from the corresponding rotation during the squat activity ($p < 0.05$). B: Femoral external rotations based on contact locations determined from MR and CT derived cartilage and bone models, respectively. There were no statistically significant differences between rotations measured by these two methods. Solid squares represent significant differences between rotations determined by the MR model based contact locations and the regid body bone motions in graph A ($p < 0.05$). Solid circles represent significant differences between rotations determined by the CT model based contact locations and the rigid body bone motions in graph A ($p < 0.05$).

similar to the "screw home" movement reported for passive knee motions.[10]

The regions used to estimate contact location were irregularly shaped for the CT models and consistently circular or elliptical for the MR models (Fig. 4). Rotations determined from the CT and MR model contact points were not significantly different (Figs. 4 and 5B). There were significant differences between rotations determined from rigid body bone kinematics and contact points for stair and squat activities at flexion angles <30° (Fig. 5A and B). There were no statistically significant differences between rotations measured by MR derived model and CT derived model.

AP translation of the condylar contact regions showed three phases over the range of motion (Fig. 6). From extension to 20° flexion, the contact points rotated externally with posterior translation. From 20° to 80°, they translated posteriorly with little additional rotation. For flexion >80° (squat and kneel), additional external rotation resulted predominantly from posterior lateral translation, essentially pivoting about the medial compartment. There were significant differences in lateral contact positions between squat and kneel from 100°–139° flexion (<0.01 for 100° to 135°, and $p = 0.015$ at 139°). There were no differences in contact positions for the medial condyle.

Condylar separation was not observed at flexion <150°. In two subjects the minimum medial surface separation exceeded 2 mm (MR cartilage model) in terminal kneeling at >150° flexion.

DISCUSSION

This study examined dynamic 3D normal knee kinematics in three activities, including two types of maximum knee flexion, using a high-resolution flat panel X-ray detector. Different values of knee axial rotation were observed with different activities, with the greatest femoral external rotation observed during the squat activity. No subluxation of the lateral femoral condyle was observed in maximum knee flexion, and condylar separation from the tibial surface was not commonly observed. Rigid body kinematics measured from bone-embedded coordinate systems produced different joint axial rotations than were measured from the orientation of the medial and lateral condylar contact locations for flexion <30°.

Knee axial rotations differed according to the method of calculation. Rotations defined from bone-embedded coordinate systems showed gradual femoral external rotation across the entire flexion arc (Fig. 5A). Rotations measured from condylar contact locations exhibited three phases: sharp external rotation from 0° to 15° flexion, relatively constant rotation from 20° to 80° flexion, and increasing rotation from 80° to 150° flexion (Fig. 5B). Significant differences in early flexion (0° to 30°) are due to femoral geometry. Iwaki et al.[11] showed that the sagittal profile of the medial femoral condyle is composed of a larger distal and smaller posterior circular arc, while the lateral condyle is well described by a single circular facet.

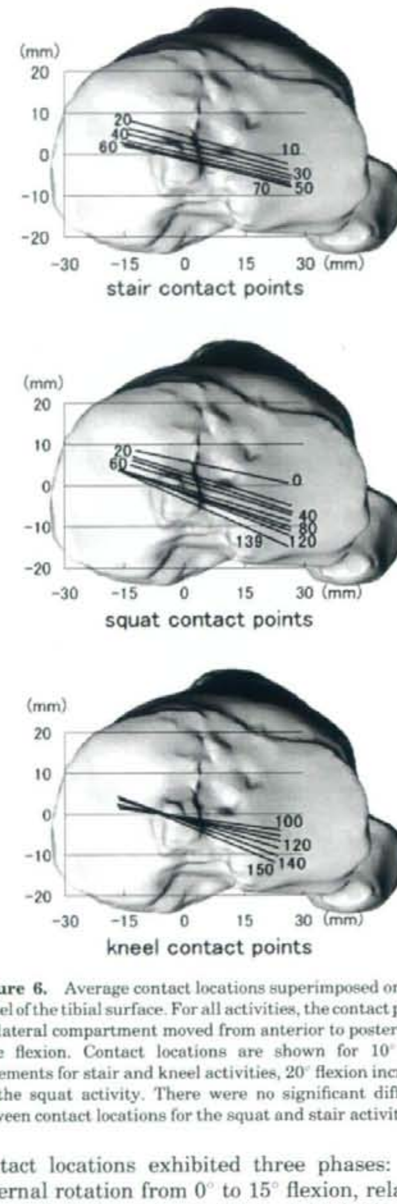

Figure 6. Average contact locations superimposed on an MR model of the tibial surface. For all activities, the contact points in the lateral compartment moved from anterior to posterior with knee flexion. Contact locations are shown for 10° flexion increments for stair and kneel activities, 20° flexion increments for the squat activity. There were no significant differences between contact locations for the squat and stair activites.